Optical response of high-T_c cuprates: Possible role of scattering rate saturation and in-plane anisotropy

N. E. Hussey, J. C. Alexander, and R. A. Cooper
H. H. Wills Physics Laboratory, University of Bristol, Tyndall Avenue, BS8 1TL, United Kingdom

(Received 15 September 2006; revised manuscript received 17 October 2006; published 15 December 2006)

We present a generalized Drude analysis of the in-plane optical conductivity $\sigma_{ab}(T,\omega)$ in cuprates taking into account the effects of in-plane anisotropy. A simple ansatz for the scattering rate $\Gamma(T,\omega)$, that includes anisotropy, a quadratic frequency dependence, and saturation at the Mott-Ioffe-Regel limit, is able to reproduce recent normal state data on an optimally doped cuprate over a wide frequency range. We highlight the potential importance of including anisotropy in the full expression for $\sigma_{ab}(T,\omega)$ and challenge previous determinations of $\Gamma(\omega)$ in which anisotropy was neglected and $\Gamma(\omega)$ was indicated to be strictly linear in frequency over a wide frequency range. Possible implications of our findings for understanding thermodynamic properties and self-energy effects in high-T_c cuprates will also be discussed.

DOI: 10.1103/PhysRevB.74.214508 PACS number(s): 74.72.Hs, 74.25.Gz, 74.25.Fy, 72.10.−d

I. INTRODUCTION

The normal state charge dynamics of cuprate superconductors, both in- and out-of-plane, are still poorly understood despite two decades of intensive research.[1] While the experimental situation is now well established, its theoretical interpretation remains controversial, largely due to the high transition temperatures themselves restricting the temperature range over which individual models can be critically examined. In this regard, measurements of the in-plane optical conductivity $\sigma_{ab}(T,\omega)$ play a central role. The ability to resolve small spectral weight differences between the normal and superconducting state (the so-called Ferrell-Glover-Tinkham sum rule) is testimony to the improvement in quality of optical conductivity data (and its analysis) in recent years.[2–4] This has also led to an extension of the energy scale (up to the bare bandwidth W) over which information on the quasiparticle response can be determined, thus further constraining theory and allowing the possibility to distinguish between the various phenomenologies proposed.

Historically, the type of approach employed to analyze the optical conductivity data for a particular sample has depended on where it resides in the cuprate phase diagram. In low-doped cuprates, i.e., near half-filling, it has become customary to adopt the so-called two-component picture that assumes a Drude component at low frequencies coupled with a Lorentzian in the mid-infrared region which contains a large fraction of the spectral weight.[5] In optimally and overdoped cuprates on the other hand, these two components appear to merge, making a one-component model the more appropriate. In this case, one uses the so-called extended or generalized Drude model[6] that assumes a single Drude component for $\omega < W$ but with a scattering rate $\Gamma(T,\omega)$ and coupling constant $\lambda(T,\omega)$ showing strong frequency dependence. In this case,

$$\sigma(T,\omega) = \frac{\Omega_p^2/4\pi}{\Gamma(T,\omega) - i\omega[1+\lambda(T,\omega)]} \quad (1)$$

where Ω_p is the plasma frequency and $\lambda(T,\omega)$ is causally related to $\Gamma(T,\omega)$ via the Kramers-Kronig transformation

$$\lambda(T,\omega) = \frac{2}{\pi} P \int_0^\infty \frac{\Gamma(T,\Omega)}{\Omega^2 - \omega^2} \mathrm{d}\Omega. \quad (2)$$

Here P stands for the Cauchy principal value. To extract $\Gamma(T,\omega)$, it is common practice simply to invert Eq. (1), i.e.,

$$\Gamma(T,\omega) = \frac{\Omega_p^2}{4\pi} \mathrm{Re}\left[\frac{1}{\sigma(T,\omega)}\right]. \quad (3)$$

Although a consensus has not yet been reached on its overall applicability,[7] the generalized Drude approach can in principle provide valuable spectroscopic information on $\Gamma(T,\omega)$ and $\lambda(T,\omega)$, the optical analogs of the real and imaginary parts of the quasiparticle self-energy. In *optimally doped* cuprates, $\Gamma(\omega)$ extracted in this way is invariably found to be linear in frequency below 3000 cm^{-1}.[8–12] Such behavior is exemplified by recent state-of-the-art optical data on optimally doped $Bi_2Sr_2Ca_{0.92}Y_{0.08}Cu_2O_8$ (Y-Bi2212) reproduced in Fig. 1.[11] This linear dependence of $\Gamma(\omega)$ mirrors the ubiquitous T-linear resistivity in optimally doped material that extends in some cases up to 1000 K.[13] Such linearity in both frequency and temperature is consistent with a marginal Fermi-liquid (MFL) self-energy.[14] It is argued in Ref. 11 that the Y-Bi2212 data obey quantum critical scaling (though not of the MFL form) and more recently, a similar but revised scaling analysis has been carried out by the same group for the trilayer compound $Bi_2Sr_2Ca_2Cu_3O_{10}$.[15]

One of the primary objectives of the present work is to sound a note of caution for conclusions drawn using Eq. (3), the validity of which relies on all parameters in (3) being isotropic. Over the last decade, evidence has accumulated for a very significant basal-plane anisotropy in cuprates both in the quasiparticle velocity v_F and its lifetime τ, first from measurements of interlayer magnetoresistance[16] and subsequently (and more directly) from angle-resolved photoemission spectroscopy (ARPES).[17] Moreover if this anisotropy is energy dependent, what one actually obtains from plotting $\Gamma(T,\omega) \sim \mathrm{Re}[1/\sigma(T,\omega)]$ is the T- and ω-dependent Γ embracing a global angular average of the anisotropic parts of $\Gamma(\phi,T,\omega)$, $\lambda(\phi,T,\omega)$, $v_F(\phi)$, and the in-plane Fermi wave vector $k_F(\phi)$. Hence, all anisotropy *together with its frequency dependence* is being subsumed into $\Gamma(\omega)$. We argue

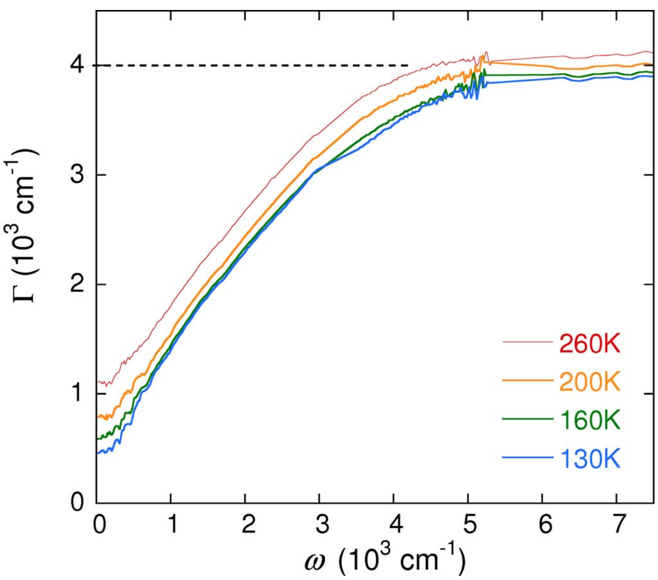

FIG. 1. (Color online) $\Gamma(T,\omega)$ extracted from Eq. (3) for optimally doped Y-Bi2212. The dashed line represents the value $\Gamma_{sat} = 4000\ \mathrm{cm}^{-1} \sim 0.5$ eV at which $\Gamma(T,\omega)$ saturates. Data reproduced from Ref. 11 by kind permission of D. van der Marel.

here that a more rigorous way to model the data is to use the fully anisotropic expression for $\sigma_{ab}(T,\omega)$ within an extended Drude formalism. As we shall show, employing the data of Ref. 11 for illustration, this can have a profound effect upon the extracted frequency dependence of $\Gamma(\omega)$.

As seen in Fig. 1, $\Gamma(\omega)$ in Y-Bi2212 starts to deviate from linearity at frequencies above 3000 cm^{-1}, tending to a constant value $\Gamma_{sat} \sim 4000$ cm^{-1}. Such "saturation" in $\Gamma(T,\omega)$ is suggestive of strong coupling to bosons rather than critical scaling phenomena, though given the high frequency at which saturation sets in (~ 5000 cm^{-1}), presumably not of coupling to phonons. Recently, Norman and Chubukov[18] showed that a model based on coupling to a broad spectrum (there presumed to be of spin fluctuations) extending out to 0.3 eV captures most of the essential features of the data in Ref. 11, although a gapped MFL model also gave similarly good agreement.

One aspect of the data in Fig. 1 however, appears at odds with the standard picture of electron-boson coupling. According to the standard Allen formalism,[19,20] saturation of $\Gamma(\omega)$ sets in at progressively higher frequencies as T is raised, more so still if the bosonic response were to broaden and shift to higher frequencies, as is expected if the strongest coupling is to antiferromagnetic spin fluctuations. The data however, do *not* show this tendency; if anything $\Gamma(\omega)$ saturates at a *lower* frequency as T increases. This counter trend in $\Gamma(T,\omega)$ is seen particularly clearly in the optical response of underdoped $Ca_{2-x}Na_xCuO_2Cl_2$.[21]

We consider an alternative physical origin for the saturation in $\Gamma(T,\omega)$, namely an asymptotic approach to the Mott-Ioffe-Regel (MIR) limit for coherent charge propagation. The MIR criterion states that the electron mean-free-path ℓ has a lower limit of order the interatomic spacing a (alternatively speaking, Γ can never exceed the bare bandwidth W).[22,23] Beyond that point, the concept of carrier velocity is lost and all coherent quasiparticle motion vanishes. Such a threshold is seen, for example, in metals exhibiting resistivity saturation, where the saturation value is found to be consistent with $\ell = a$.[24,25] The MIR limit was in fact invoked to account for the saturation of $\Gamma(\omega)$ in $Ca_{2-x}Na_xCuO_2Cl_2$.[21] In Y-Bi2212, Ω_p is estimated to be $\sim 19\,500$ cm^{-1}, which upon converting to SI units, gives $\langle v_F\rangle \sim 3.4\times 10^5$ ms^{-1} for $\langle k_F\rangle \sim 7.0$ nm^{-1} (here $\langle v_F\rangle$ and $\langle k_F\rangle$ refer to the angle-averaged bare velocity $v_F(\phi)$ and Fermi wave vector $k_F(\phi)$, respectively, the latter derived from ARPES measurements[26,27]). Taking the strict definition of the MIR criterion we thus estimate $\Gamma_{MIR} = \langle v_F\rangle / a \sim 4500$ cm^{-1} (converting back to cgs). Comparison with Fig. 1 suggests that $\Gamma_{sat} \sim \Gamma_{MIR}$, i.e., the saturation value of $\Gamma(T,\omega)$ is compatible with the MIR limit as defined. Although Γ_{sat} in Fig. 1 does show a small increase with increasing temperature ($\sim 5\%$ for $100\ \mathrm{K} \leqslant T \leqslant 300$ K), the change, as stated above, is not as much as would be expected to arise, say, from coupling to bosons.[28]

The combination of strong fourfold basal plane anisotropy and saturation of the scattering rate at the MIR limit has previously been incorporated by one of the authors into a phenomenological model, the so-called anisotropic scattering rate saturation (ASRS) model, to account for a number of anomalous in-plane transport properties of high-T_c cuprates, including the separation of transport and Hall lifetimes (at optimal doping) and modifications to Kohler's rule.[29] In this paper, we extend the ASRS model into the frequency domain using the generalized Drude approach and employ the derived expressions to fit experimental $\sigma_{ab}(T,\omega)$ data for optimally doped Y-Bi2212 over a range of temperatures. The model is found to reproduce the optical response of Y-Bi2212 over two decades in frequency with parameters that are consistent with those extracted from dc transport measurements on Bi2212.[29] Details of the mass enhancement, extracted self-consistently in the analysis, are also compared with specific heat and ARPES data in Bi-2212 with similar success.

The paper is set out as follows. The ASRS model is introduced in Sec. II and extended into the realm of finite frequencies. In Sec. III, the fitting to the experimental data on Y-Bi2212 is presented while in Sec. IV, the possible consequences for our understanding of thermodynamic properties in cuprates are discussed. Finally, we offer our summary and conclusions in Sec. V.

II. ASRS MODEL AND OPTICAL CONDUCTIVITY

The ASRS model assumes a temperature (energy) dependence which is quadratic everywhere on the Fermi surface but exhibits strong (fourfold symmetric) basal plane anisotropy. Evidence for an (approximately) quadratic temperature (energy) dependence in cuprates, extending over a wide temperature (energy) range, initially came from measurements of the inverse Hall angle cot $\theta_H(T)$ (Refs. 30–32) and more recently from ARPES studies of the self-energy near the nodal region along (π,π).[33] When combined with an appreciable elastic scattering rate that also contains fourfold anisotropy (sometimes ascribed to small angle scattering of impurities located between the CuO_2 planes[34]), the intrinsic or "ideal" scattering rate $\Gamma_{\text{ideal}}(\phi,T)$ can be written most succinctly as follows:

$$\Gamma_{\text{ideal}}(\phi,T) = \alpha(1 + c\cos^2 2\phi) + \beta(1 + e\cos^2 2\phi)T^2, \quad (4)$$

where c and e are anisotropy parameters while α and β are coefficients of the component scattering rates along (π,π). To extend the model to finite frequencies we shall simply adopt the standard Fermi-liquid condition for electron-electron scattering[35] and accordingly write $\Gamma_{\text{ideal}}(\phi,T,\omega)$,

$$\Gamma_{\text{ideal}}(\phi,T,\omega) = \alpha(1 + c\cos^2 2\phi) + \beta(1 + e\cos^2 2\phi)(T^2 + (\hbar\omega/2\pi k_B)^2). \quad (5)$$

To accommodate the MIR limit we invoke the anisotropic "parallel-resistor" formula,

$$\frac{1}{\Gamma_{\text{eff}}(\phi,T,\omega)} = \frac{1}{\Gamma_{\text{ideal}}(\phi,T,\omega)} + \frac{1}{\Gamma_{\text{MIR}}} \quad (6)$$

to mimic the form of the resistivity $\rho(T)$ found in systems exhibiting resistivity saturation.[36] (We stress here that this formula should be viewed as scattering rates adding in parallel rather than as different conduction channels.) The formula presumes that the MIR limit is manifest at all temperatures and, by extension, all energies below the bandwidth. To fit to the optical conductivity data, we further need the effective mass enhancement factor $\lambda_{\text{eff}}(\phi,T,\omega)$, obtained via the appropriate Kramers-Kronig transformation (2). To simplify our working, we make the following substitutions, $\Gamma_0=\alpha(1+c\cos^2 2\phi)$, $\Theta=\beta(1+e\cos^2 2\phi)$, $\hbar/2\pi k_B=1$ and $\Lambda=\Gamma_{\text{MIR}}+\Gamma_0+\Theta T^2$, and then rearrange Γ_{eff} as follows:

$$\Gamma_{\text{eff}}(\phi,T,\omega) = \Gamma_{\text{MIR}} - \left(\frac{\Gamma_{\text{MIR}}^2}{\Lambda + \Theta\omega^2}\right). \quad (7)$$

Thus $\lambda_{\text{eff}}(\phi,T,\omega)$ becomes:

$$\lambda_{\text{eff}}(\phi,T,\omega) = \frac{2}{\pi}P\int_0^\infty \frac{\Gamma_{\text{MIR}}}{\Omega^2-\omega^2}d\Omega - \frac{\Gamma_{\text{MIR}}^2}{\Lambda}\frac{2}{\pi}P\int_0^\infty \frac{1}{(\Omega^2-\omega^2)}\frac{1}{(1+\Theta\omega^2/\Lambda)}d\Omega. \quad (8)$$

The first integral here is zero. The second gives

$$\lambda_{\text{eff}}(\phi,T,\omega) = \Gamma_{\text{MIR}}^2\left(\frac{\Theta}{\Lambda}\right)^{1/2}\left(\frac{1}{\Lambda+\Theta\omega^2}\right). \quad (9)$$

A similar ansatz (but without anisotropy) has been used previously to replicate the form of $\Gamma(\omega)$ extracted from an extended Drude analysis for heavy fermion compounds[37] although in that case, no physical explanation for Γ_{MIR} was provided. Interestingly, when we extrapolate to $\omega=0$ and low T where $\Lambda \sim \Gamma_{\text{MIR}}$, Eq. (7) reduces to an expression for the dc mass enhancement factor, $\lambda_{\text{eff}}(0) \sim (\hbar\Theta\Gamma_{\text{MIR}}/4\pi^2 k_B)^{1/2} \sim (\hbar\Theta\langle v_F\rangle/4\pi^2 a k_B)^{1/2}$. This expression (in its isotropic form) has been shown to give a reliable estimate of the A coefficient of the T^2 resistivity found in a variety of strongly correlated metals.[38]

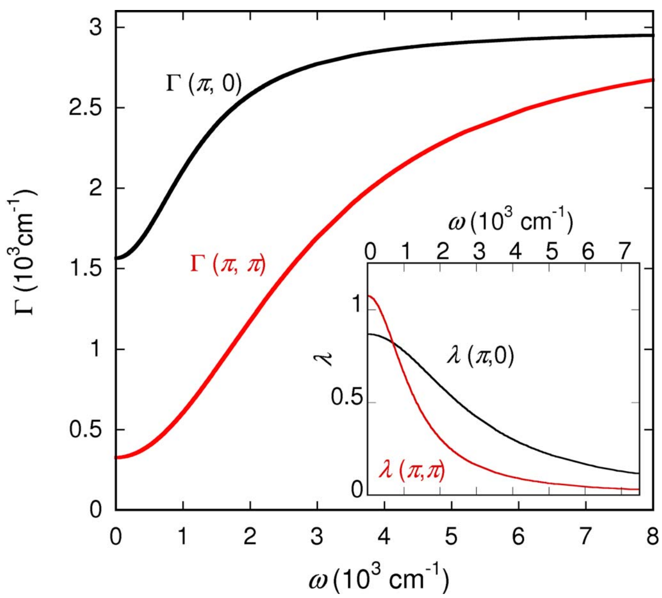

FIG. 2. (Color online) $\Gamma_{\text{eff}}(\omega)$ along (π,π), (red) and $(\pi,0)$, (black) at $T=200$ K according to the ASRS phenomenology. Inset: Corresponding $\lambda_{\text{eff}}(\omega)$ for the same two orientations, obtained via the appropriate Kramers-Kronig transformation.

Figure 2 shows the evaluated frequency-dependent ASRS scattering rate $\Gamma_{\text{eff}}(\omega)$ along (π,π), (red line) and $(\pi,0)$, (black line). (In this example, the parameters used are the same as those used in Fig. 3 below to fit the 200 K data). The corresponding mass enhancement factors $\lambda_{\text{eff}}(\omega)$ are shown in the inset. One should note that even though the anisotropy in $\Gamma_{\text{ideal}}(\phi)$ is large ($e=9$ in the example shown), the effective anisotropy in $\Gamma_{\text{eff}}(\omega=0)$ is significantly less so ($\sim$5). Moreover the anisotropy in $\lambda_{\text{eff}}(\omega=0)$ is inverted with respect to $\Gamma_{\text{eff}}(\omega=0)$. Both of these features are due to the presence of Γ_{MIR} which acts to "dampen" the intrinsic anisotropy in the interaction strength. Note too that $\Gamma_{\text{eff}}(\omega)$ along $(\pi,0)$ saturates at a much lower frequency than occurs along

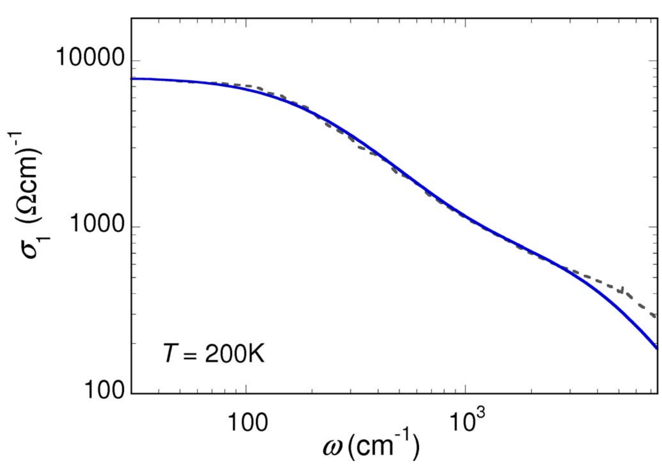

FIG. 3. (Color online) $\sigma_1(\omega)$ data (dashed gray line) and fit (solid blue line) at $T=200$ K. Fitting parameters are $\alpha=64$ cm^{-1}, $\beta=0.0072$ cm^{-1}/K^2, $c=3$, and $e=9$.

(π,π) and at high frequencies, the two scattering rates converge, as one should expect through the averaging of k states.

Finally, we insert (5), (6), and (9) into the full expression for the real part of the conductivity $\sigma_1(T,\omega)=\mathrm{Re}[\sigma_{ab}(T,\omega)]$ for a two-dimensional Fermi surface where

$$\sigma_{ab}(T,\omega)=\frac{e^2}{4\pi^3\hbar}\left(\frac{2\pi}{d}\right)\int_0^{2\pi}\frac{k_F(\phi)v_F(\phi)\cos^2(\phi-\gamma)}{\cos\gamma}\times\frac{d\phi}{\Gamma_{\mathrm{eff}}(\phi,T,\omega)-i\omega[1+\lambda_{\mathrm{eff}}(\phi,T,\omega)]}. \quad (10)$$

(For a derivation of this expression in the $\omega=0$ limit see the Appendix of Ref. 29.) Here d is the lattice spacing and ϕ is taken around the two-dimensional projection of the CuO_2 Fermi surface. $\gamma=\tan^{-1}[\partial/\partial\phi(\log k_F(\phi))]$ is the angle between v_F and dk_r (the infinitesimal vector element along k_F). While this Boltzmann-type approach cannot be applicable over the entire energy range, we believe the formalism presented here adequately represents the main issue regarding anisotropy and that the results will not differ significantly from those which would be extracted via a more precise Kubo formalism.[39]

III. RESULTS

In order to minimize the number of fitting parameters, we have fixed both $k_F(\phi)$ and $v_F(\phi)$ using the tight-binding expression[26] for the CuO_2 plane (bonding) band in Bi2212 (Ref. 40) and set $\Gamma_{\mathrm{MIR}}=\langle v_F\rangle/a$. Hence the only free parameters in our fitting procedure are the coefficients in our expression for $\Gamma_{\mathrm{ideal}}(\phi,T,\omega)$, namely α and β, c and e. Figure 3 shows our fit to $\sigma_1(\omega)$ at $T=200$ K. The fitting parameters are listed in the figure caption. The ASRS parametrization provides an excellent fit to the experimental data from the lowest frequencies studied up to $\omega\sim 3000$ cm^{-1}. Note that no scaling factors were applied in this fitting procedure. The deviation of the fit above 3000 cm^{-1} is most probably due to the fact that the magnitude of $\langle v_F\rangle$ from tight binding which was used to fix Γ_{MIR} is somewhat lower than that estimated from the optical data.

To track the evolution of $\sigma_1(T,\omega)$ for all $T>T_c$, we simply insert the relevant temperature into (5) keeping all other parameters in (10) fixed. The fittings are shown in Fig. 4. The evolution of the low-frequency response in particular is reproduced well by the parametrization. Similarly good fits were obtained too for $\sigma_2(T,\omega)$, the imaginary part of the conductivity and also for the phase-angle φ (not shown), though given their mutual interdependence via the Kramers-Kronig relations, this is not so surprising.

The dc transport properties can be derived within the same parametrization scheme (Ref. 29),

$$\rho_{ab}(T)=\frac{1}{\sigma_{ab}(T,\omega=0)}, \quad (11)$$

$$\tan\Theta_H(T)=\frac{\sigma_{xy}(T)}{\sigma_{ab}(T,\omega=0)}, \quad (12)$$

where

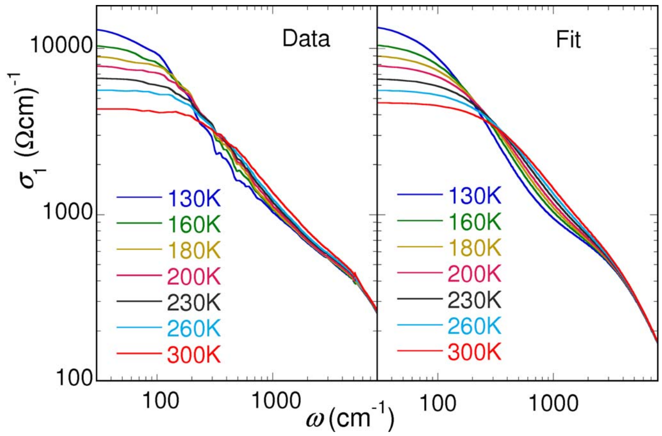

FIG. 4. (Color online) $\sigma_1(\omega)$ data (left panel) and fit (right panel) for a range of temperatures 130 K$\leqslant T\leqslant$300 K. In this fitting routine, all fitting parameters were fixed to their value(s) at 200 K.

$$\sigma_{xy}(T)=\frac{-e^3B}{4\pi^3\hbar^2}\left(\frac{2\pi}{d}\right)\times\int_0^{2\pi}\frac{v_F(\phi)\cos(\phi-\gamma)}{\Gamma_{\mathrm{eff}}(\phi,T,\omega=0)}\frac{\partial}{\partial\phi}\left(\frac{v_F(\phi)\sin(\phi-\gamma)}{\Gamma_{\mathrm{eff}}(\phi,T,\omega=0)}\right)\mathrm{d}\phi. \quad (13)$$

Figure 5 shows the resultant simulation plots of $\rho_{ab}(T)$ and cot $\theta_{\mathrm{H}}(T)$ in the temperature interval $0\leqslant T\leqslant 600$ K. The region between 100 and 400 K is shown as a thick solid line for emphasis. Over this latter temperature range $\rho_{ab}(T)$ is found to vary linearly with temperature (as indicated by the dashed line) but displays clear upward curvature at lower temperatures as $\rho_{ab}(T)$ approaches a finite *positive* intercept. Above 400 K, $\rho_{ab}(T)$ starts to deviate from linearity as it approaches the saturation value assumed by the model. The fact that $\rho_{ab}(T)$ in optimally doped cuprates follows a T-linear dependence up to much higher temperatures and values *beyond* the MIR limit, without showing any sign of saturation, may appear at first sight to invalidate the model. Optical conductivity measurements in cuprates at elevated temperatures however, have shown evidence for a shift in the low-frequency spectral (Drude) weight above 300 K suggesting some form of thermally induced decoherence of the quasiparticles.[25,41] The vanishing of the zero-frequency Drude peak also implies that the continuation of the T-linear dependence of $\rho_{ab}(T)$ beyond the MIR limit cannot be associated with an unbounded escalation of the (T-linear) scattering rate. This conjecture is further supported by the observation of saturation of $\Gamma(T,\omega)$ at high frequencies at a value $\Gamma_{\mathrm{sat}}\sim\Gamma_{\mathrm{MIR}}\sim W$ (see Fig. 1).

In contrast to the T linearity of $\rho_{ab}(T)$, cot $\theta_{\mathrm{H}}(T)$ is found to follow the form $A+BT^n$ between T_c and 400 K, with $n=1.75$. This unusual power law is remarkably similar to that observed experimentally ($n=1.78$) in thin films of optimally doped Bi2212.[42] The origin of the so-called "separation of lifetimes"[43] governing $\rho_{ab}(T)$ and cot $\theta_{\mathrm{H}}(T)$ in cuprates has been a long-standing controversy.[1] In single lifetime models with a strongly anisotropic $\ell(\mathbf{k})$, the Hall conductivity as given in Eq. (13) is dominated by those quasiparticles with

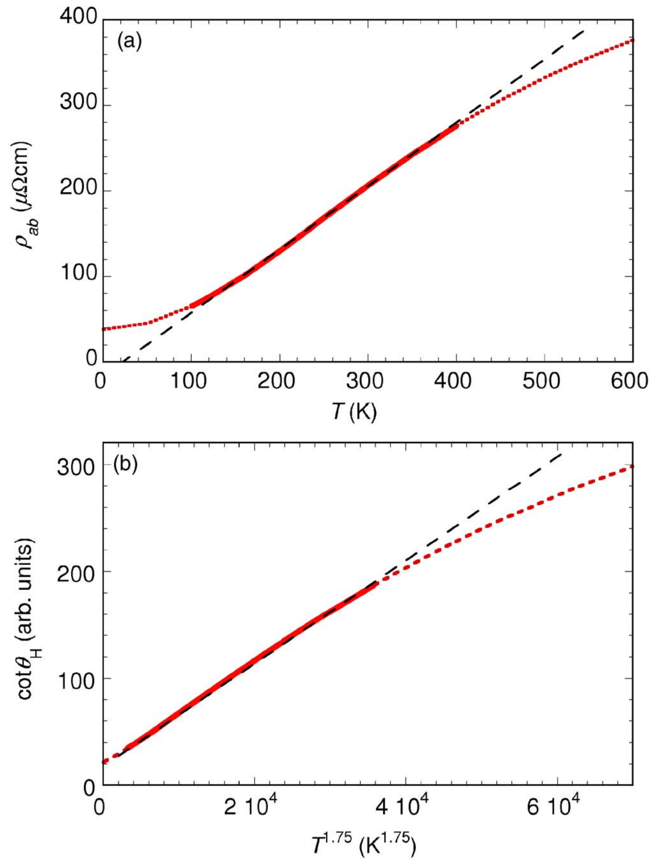

FIG. 5. (Color online) (a) $\rho_{ab}(T)$ extracted from the fitting parameters listed in the figure caption of Fig. 3. (b) Corresponding cot $\theta_H(T)$ versus $T^{1.75}$ for the same fitting parameters. The thick solid lines highlight the region between 100 and 400 K where $\rho_{ab}(T)$ is T linear and cot $\theta_H(T) \sim A + BT^{1.75}$. The dashed lines are guides to the eye.

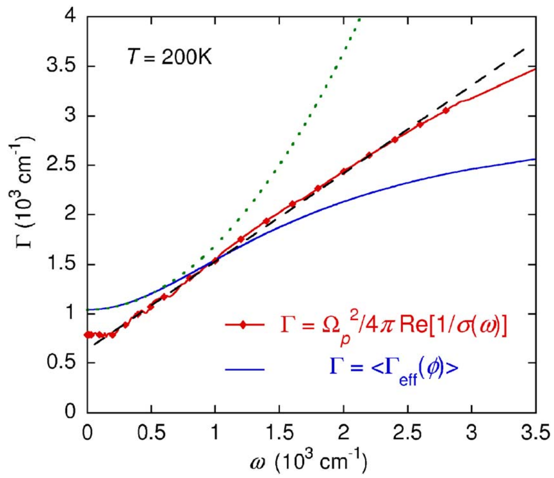

FIG. 6. (Color online) Comparison between $\Gamma(\omega)$ obtained from Eq. (3) (solid red line with diamonds) and the angle-averaged $\Gamma_{eff}(\omega) = (1/2\pi)\oint \Gamma_{eff}(\phi,\omega)d\phi$ extracted from the fitting parameters (solid blue line). The dotted and dashed lines are quadratic and linear extrapolations up from the respective low-frequency limits.

the longest mean-free-path.[44] In optimally doped cuprates, the T dependence of cot θ_H would thus be determined by the nodal quasiparticles near (π,π) which present a near-quadratic temperature (and frequency) dependence. $\rho_{ab}(T)$ on the other hand, is a global average of $\Gamma_{eff}(\phi,T)$ and since the antinodal saddle regions near $(\pi,0)$ exhibit a *sub*linear, almost flat T dependence, the integral over the entire Fermi surface would yield $\rho_{ab}(T) \sim T$. Comparable considerations led Ioffe and Millis to develop their widely regarded "cold-spots" model for high-T_c cuprates.[45]

Let us now examine how the anisotropy becomes reflected in the form of $\Gamma(\omega)$ and vice versa. In Fig. 6, the solid red line with diamonds represents $\Gamma(\omega)$ at T=200 K as determined by Eq. (3), i.e., just the inversion of the (isotropic) conductivity, below 3500 cm^{-1}. As described in Ref. 11 *and many other papers adopting the same procedure*, $\Gamma(\omega)$ appears linear below 3000 cm^{-1} (thick dashed line). The solid blue line in Fig. 6 is the angle-averaged $\langle\Gamma_{eff}(\omega)\rangle = (1/2\pi)\oint\Gamma_{eff}(\phi,\omega)d\phi$ where $\Gamma_{eff}(\phi,\omega)$ is the ASRS scattering rate inserted into the full anisotropic expression (10) along with $\lambda_{eff}(\phi,\omega)$ and the anisotropic Fermi surface parameters. Note now that $\Gamma_{eff}(\omega) \propto \omega^2$ up to 800 cm^{-1} (dotted line) and that the ω-linear regime is restricted to a narrow crossover region between the ω^2 low-frequency response and the onset of saturation. The key point to make here is that *both* parametrizations, the one isotropic, the other anisotropic, can fit the optical conductivity data equally well in this frequency range, and yet the form of $\Gamma(\omega)$ is markedly different in the two cases. Of course, our modeling does not rule out a contribution to $\Gamma(\omega)$ that is intrinsically ω linear; it merely highlights the fact that when neglecting anisotropy one is going to infer information about $\Gamma(\omega)$ solely from the (ω linear) frequency dependence of Re$[1/\sigma(\omega)]$ without any physical justification for doing so.

IV. DISCUSSION

In this section we discuss some of the implications of the above modeling beyond the inherent form of $\Gamma(\omega)$. One immediate consequence of our assumption that Γ_{MIR} constitutes a ceiling on $\Gamma(\omega)$ is the reduction in $\lambda_{eff}(0)$ with increasing temperature. Due to the Kramers-Kronig relation, $\lambda_{eff}(0)$ is governed to a large degree by the *difference* between the low and high frequency limits of $\Gamma(\omega)$. As the temperature rises, $\Gamma(\omega=0)$ quickly rises due to the increase in inelastic scattering. Γ_{MIR} on the other hand is independent of temperature (if one ignores the effects of thermal expansion and T-induced variations in the band dispersion). $\Gamma(\omega)$ is thus confined by these two limiting extremes, leading to an overall reduction in $\lambda_{eff}(0)$. Since $\lambda_{eff}(0)$ governs the mass enhancement, the effect should be manifest in thermodynamic properties such as the electronic specific heat coefficient $\gamma_0(T)$. Figure 7 shows the T dependence of the (angle-averaged) $\lambda_{eff}(0)$ and γ_0 derived from our modeling of the optical data assuming a band mass m_b=1. $\gamma_0(T)$ is seen to rise by approximately 50% as the temperature falls from 300 to 100 K. Both the magnitude of γ_0 and its variation with temperature are in reasonable agreement with measured data on Bi2212.[46] Within the standard Allen formalism,[19] $\lambda_{eff}(0)$ should be essentially T

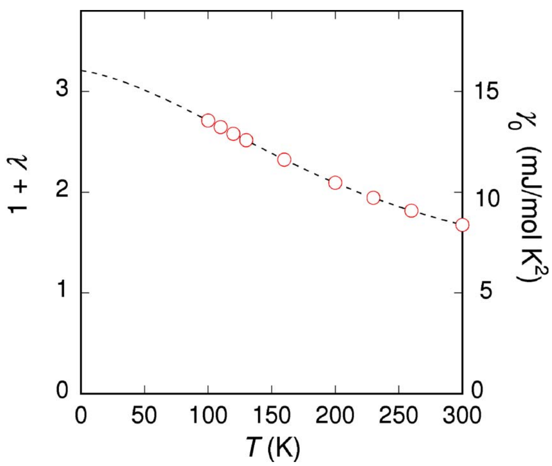

FIG. 7. (Color online) T dependence of the mass enhancement $1+\lambda_{\text{eff}}$ as extracted from the fitting parameters of model 1. The axis labels on the right-hand side correspond to the electronic specific heat coefficient γ_0 assuming a band mass $m_b=1$.

independent if phonons provide the dominant interaction [otherwise $\rho(T)$ in a standard metal would deviate from its strictly T-linear temperature dependence]. Within a spin fluctuation picture, one could expect by contrast $\lambda_{\text{eff}}(0)$ and hence $\gamma_0(T)$ to fall with increasing temperature as the low-frequency susceptibility is wiped out. However, as we have already argued, within the same scenario one should expect the onset of saturation in $\Gamma(\omega)$ to shift to higher frequencies with increasing temperature, which to our knowledge has never been observed experimentally.

One can also compare the mass enhancement of the optical (particle-particle) self-energy to that of the single-particle self-energy $\Sigma(\omega)$ derivable from ARPES along the different k-space directions. Along (π,π), for example, $\partial\,\text{Re}\,\Sigma/\partial\omega \sim 1.9$ for slightly underdoped Bi-2212 at $T=130$ K.[47] According to our fitting of the optical data, we obtain $\lambda_{\text{eff}}(0)=1.5$ along (π,π) at the same temperature, giving $1+\lambda_{\text{eff}}(0) > \partial\,\text{Re}\,\Sigma/\partial\omega$ at (π,π). This inequality suggests that (current-current) vertex corrections do play some role in the physics of the nodal regions. What the ARPES data of Ref. 45 do *not* show is the tendency toward saturation in $\text{Im}\,\Sigma(\omega)$, a key component of the ASRS phenomenology. However, a recent ARPES study of the single-layer Bi-compound $Bi_{1.74}Pb_{0.38}Sr_{1.88}CuO_{6+\delta}$ has revealed that at higher energies, there is evidence for saturation of $\text{Im}\,\Sigma(\omega)$ at values comparable to the bandwidth.[48] It would be interesting in due course to examine whether the phenomenology presented here could also be applied to explain the form of the single-particle self-energy.

V. CONCLUSIONS

In this paper, we have sought to counter the ubiquitous use of Eq. (3) in extraction of $\Gamma(\omega)$ from the in-plane normal-state optical data of high-T_c cuprates. We have also demonstrated how basal-plane anisotropy in the scattering rate, ignored until now in the analysis of $\sigma_{ab}(\omega)$, can bring about a marked change in the analytical form of $\Gamma(\omega)$; most strikingly, the customary linear frequency dependence at low ω is seen as being an artifact of a fitting routine that presumes isotropic scattering. The key take-home message is that the intrinsic low energy response of optimally doped cuprates is only able to be properly determined once all anisotropic factors are fully taken into account. Because the system contains very significant anisotropy which may vary with frequency, one cannot use (3) ubiquitously to extract $\Gamma(\omega)$ from $\sigma_{ab}(\omega)$. We have argued that a more rigorous way to proceed is to input a form of $\Gamma(\phi,T,\omega)$ into the full anisotropic expression for $\sigma_{ab}(\omega)$ which in conjunction with its Kramers-Kronig partner $\lambda(\phi,T,\omega)$ and the correct Fermi surface parametrization would fit the data.

Above we have proposed one such parametrization, based on a $\Gamma(\omega)$ with a quadratic frequency dependence, strong basal-plane anisotropy, and a tendency toward saturation at the MIR limit, which secures a good account of the optical response. Moreover, we have indicated how the same parametrization can account for other physical properties such as anomalies in the dc transport and the specific heat. The ASRS phenomenology presented here clearly is not the whole story however. While there is a growing body of evidence for saturation and a quadratic frequency dependence in cuprates, particularly along the nodal direction, there is mounting evidence too for some form of strong bosonic feature in the antinodal regions near the Brillouin zone boundaries,[49–51] the origin of which remains controversial.[52–54] This contribution to $\Gamma(\phi,T,\omega)$ should also be explored within the present phenomenology for completeness. What we would argue however, is that since scattering is already so intense at $(\pi,0)$, the true, ideal form of $\Gamma(\omega)$ [and $\text{Im}\,\Sigma(\omega)$] in this region of the Brillouin zone inevitably will be significantly renormalized due to the overarching presence of Γ_{MIR}, masking the inherent nature of $\Gamma(\omega)$ in many of the physical properties that are measured. This may help to explain why it has taken the community so long to reach a consensus on the various interactions and scattering mechanisms that influence the self-energy of the in-plane antinodal quasiparticles in the cuprates and which ultimately, may drive high temperature superconductivity. Finally, for a complete formulation of the physics of cuprates to emerge, a number of the issues raised in the present work will have to be addressed. In particular, we have shown that saturation of the frequency dependent scattering rate at the MIR limit greatly influences the transport behavior in cuprates over a very wide energy scale and to acknowledge its presence may turn out to be a key step in the development of a coherent description of the charge dynamics there.

ACKNOWLEDGMENTS

The authors would like to acknowledge stimulating and enlightening discussions with N. Bontemps, A. V. Chubukov, R. P. S. M. Lobo, D. B. Tanner, T. Timusk, and D. van der Marel. The authors would especially like to thank D. van der Marel for making his optical data available to us for this analysis and J. A. Wilson for a critical reading of the manuscript.

[1] N. E. Hussey in *Treatise on High Temperature Superconductivity* edited by J. R. Schrieffer (Springer-Verlag, Amsterdam, 2006), and references therein.

[2] H. J. A. Molegraaf, C. Presura, D. van der Marel, P. H. Kes, and M. Li, Science **295**, 2239 (2002).

[3] A. F. Santander-Syro, R. P. S. M. Lobo, N. Bontemps, Z. Konstantinovic, Z. Z. Li, and H. Raffy, Europhys. Lett. **62**, 568 (2003).

[4] A. V. Boris, N. N. Kovaleva, O. V. Dolgov, T. Holden, C. T. Lin, B. Keimer, and C. Bernhard, Science **304**, 708 (2004).

[5] D. N. Basov, and T. Timusk, Rev. Mod. Phys. **77**, 721 (2005).

[6] J. W. Allen, and J. C. Mikkelsen, Phys. Rev. B **15**, 2952 (1977).

[7] D. B. Tanner, H. L. Liu, M. A. Quijada, A. M. Zibold, H. Berger, R. J. Kelley, M. Onellion, F. C. Chou, D. C. Johnston, J. P. Rice, D. M. Ginsberg, and J. T. Markert, Physica B **244**, 1 (1998).

[8] D. N. Basov, R. Liang, B. Dabrowski, D. A. Bonn, W. N. Hardy, and T. Timusk, Phys. Rev. Lett. **77**, 4090 (1996).

[9] M. A. Quijada, D. B. Tanner, R. J. Kelley, M. Onellion, H. Berger, and G. Margaritondo, Phys. Rev. B **60**, 14917 (1999).

[10] J. J. Tu, C. C. Homes, G. D. Gu, D. N. Basov, and M. Strongin, Phys. Rev. B **66**, 144514 (2002).

[11] D. van der Marel, H. J. A. Molegraaf, J. Zaanen, Z. Nussinov, F. Carbone, A. Damascelli, H. Eisaki, M. Greven, P. H. Kes, and M. Li, Nature (London) **425**, 271 (2003).

[12] Y. C. Ma and N. L. Wang, Phys. Rev. B **72**, 104518 (2005).

[13] M. Gurvitch and A. T. Fiory, Phys. Rev. Lett. **59**, 1337 (1987).

[14] C. M. Varma, P. B. Littlewood, S. Schmitt-Rink, E. Abrahams, and A. E. Ruckenstein, Phys. Rev. Lett. **63**, 1996 (1989).

[15] D. van der Marel, F. Carbone, A. B. Kuzmenko, and E. Giannini, cond-mat/0604037 (unpublished).

[16] N. E. Hussey, J. R. Cooper, J. M. Wheatley, I. R. Fisher, A. Carrington, A. P. Mackenzie, C. T. Lin, and O. Milat, Phys. Rev. Lett. **76**, 122 (1996).

[17] T. Valla, A. V. Fedorov, P. D. Johnson, Q. Li, G. D. Gu, and N. Koshizuka, Phys. Rev. Lett. **85**, 828 (2000).

[18] M. R. Norman and A. V. Chubukov, Phys. Rev. B **73**, 140501(R) (2006).

[19] S. V. Shulga, O. V. Dolgov, and E. G. Maksimov, Physica C **178**, 266 (1991).

[20] P. B. Allen, Phys. Rev. B **3**, 305 (1971).

[21] K. Waku, T. Katsufuji, Y. Kohsaka, T. Sasagawa, H. Takagi, H. Kishida, H. Okamoto, M. Azuma, and M. Takano, Phys. Rev. B **70**, 134501 (2004).

[22] A. F. Ioffe and A. R. Regel, Prog. Semicond. **4**, 237 (1960).

[23] N. F. Mott, Philos. Mag. **26**, 1015 (1972).

[24] O. Gunnarsson, M. Calandra, and J. E. Han, Rev. Mod. Phys. **75**, 1085 (2003).

[25] N. E. Hussey, K. Takenaka, and H. Takagi, Philos. Mag. **84**, 2847 (2004).

[26] M. Eschrig and M. R. Norman, Phys. Rev. B **67**, 144503 (2003).

[27] A. Kaminski, H. M. Fretwell, M. R. Norman, M. Randeria, S. Rosenkranz, U. Chatterjee, J. C. Campuzano, J. Mesot, T. Sato, T. Takahashi, T. Terashima, M. Takano, K. Kadowaki, Z. Z. Li, and H. Raffy, Phys. Rev. B **71**, 014517 (2005).

[28] In a recent optical study of heavily underdoped $YBa_2Cu_3O_{6.5}$, $\Gamma(\omega)$ was also found to be insensitive to temperature at high frequencies. This was attributed to a combination of two contributions from the spin fluctuation spectrum, one of which (the resonance mode) lost its intensity sharply with increasing temperature, J. Hwang, J. Yang, T. Timusk, S. G. Sharapov, J. P. Carbotte, D. A. Bonn, R. Liang, and W. N. Hardy, Phys. Rev. B **73**, 014508 (2006). Such a strong resonance mode is not observed in the normal state of optimally doped cuprates.

[29] N. E. Hussey, Eur. Phys. J. B **31**, 495 (2003).

[30] T. R. Chien, Z. Z. Wang, and N. P. Ong, Phys. Rev. Lett. **67**, 2088 (1991).

[31] A. Carrington, A. P. Mackenzie, C. T. Lin, and J. R. Cooper, Phys. Rev. Lett. **69**, 2855 (1992).

[32] T. Manako, Y. Kubo, and Y. Shimakawa, Phys. Rev. B **46**, 11019 (1992).

[33] A. A. Kordyuk, S. V. Borisenko, A. Koitzsch, J. Fink, M. Knupfer, B. Buchner, H. Berger, G. Margaritondo, C. T. Lin, B. Keimer, S. Ono, and Y. Ando, Phys. Rev. Lett. **92**, 257006 (2004).

[34] E. Abrahams and C. M. Varma, Proc. Natl. Acad. Sci. U.S.A. **97**, 5714 (2000).

[35] R. N. Gurzhi, Zh. Eksp. Teor. Fiz. **35**, 965 (1958) [Sov. Phys. JETP **8**, 673 (1959)].

[36] H. Wiesmann, M. Gurvitch, H. Lutz, A. K. Ghosh, B. Schwarz, M. Strongin, P. B. Allen, and J. W. Halley, Phys. Rev. Lett. **38**, 782 (1977).

[37] P. E. Sulewski, A. J. Sievers, M. B. Maple, M. S. Torikachvili, J. L. Smith, and Z. Fisk, Phys. Rev. B **38**, 5338 (1988).

[38] N. E. Hussey, J. Phys. Soc. Jpn. **74**, 1107 (2005).

[39] P. B. Allen, cond-mat/0407777 (unpublished).

[40] The tight-binding expressions can be approximated by $k_F(\phi) = 7.0(1-0.05\cos 4\phi+0.007\cos 8\phi)$ nm^{-1} and $v_F(\phi)=2.25(1-0.63\cos 4\phi-0.05\cos 8\phi)\times 10^5$ ms^{-1}. Note the corresponding $\langle v_F\rangle$ is lower than that derived from the optical plasma frequency by a factor of 0.75. Tight-binding fits also tend to overestimate the true anisotropy in $v_F(\phi)$ and so for completeness, we also considered a second parametrization using $v_F(\phi) = 2.5(1+0.5\sin^2 2\phi)\times 10^5$ ms^{-1} that is closer to the real $v_F(\phi)$ inferred from ARPES (see, for example, Ref. 27). The parameters obtained from the two models however, turn out to be very similar implying that none of the conclusions are significantly affected by our choice of $v_F(\phi)$.

[41] J. Merino and R. H. McKenzie, Phys. Rev. B **61**, 7996 (2000).

[42] Z. Konstantinovic, Z. Z. Li, and H. Raffy, Phys. Rev. B **62**, R11989 (2000).

[43] P. W. Anderson, Phys. Rev. Lett. **67**, 2092 (1991).

[44] This condition was first pointed out by Ong who showed that for a two-dimensional metal, the Hall conductivity is given by the "Stokes area" traced out by $\ell(\mathbf{k})$ within the conducting plane. N. P. Ong, Phys. Rev. B **43**, 193 (1991).

[45] L. B. Ioffe and A. J. Millis, Phys. Rev. B **58**, 11631 (1998).

[46] J. W. Loram, J. Luo, J. R. Cooper, W. Y. Liang, and J. L. Tallon, J. Phys. Chem. Solids **62**, 59 (2001).

[47] A. A. Kordyuk, S. V. Borisenko, A. Koitzsch, J. Fink, M. Knupfer, and H. Berger, Phys. Rev. B **71**, 214513 (2005).

[48] B. P. Xie, K. Yang, D. W. Shen, J. F. Zhao, H. W. Ou, J. Wei, S. Y. Gu, M. Arita, S. Qiao, H. Namatame, M. Taniguchi, N. Kaneko, H. Eisaki, Z. Q. Yang, and D. L. Feng, cond-mat/0607450 (unpublished).

[49] T. K. Kim, A. A. Kordyuk, S. V. Borisenko, A. Koitzsch, M. Knupfer, H. Berger, and J. Fink, Phys. Rev. Lett. **91**, 167002 (2003).

[50] T. Cuk, F. Baumberger, D. H. Lu, N. Ingle, X. J. Zhou, H. Eisaki, N. Kaneko, Z. Hussain, T. P. Devereaux, N. Nagaosa, and

Z.-X. Shen, Phys. Rev. Lett. **93**, 117003 (2004).
[51] M. Abdel-Jawad, M. P. Kennett, L. Balicas, A. Carrington, A. P. Mackenzie, R. H. McKenzie, and N. E. Hussey, Nat. Phys. **2**, 821 (2006).
[52] J. A. Wilson, Philos. Mag. **84**, 2183 (2004).
[53] T. P. Devereaux, T. Cuk, Z. X. Shen, and N. Nagaosa, Phys. Rev. Lett. **93**, 117004 (2004).
[54] S. V. Borisenko, A. A. Kordyuk, T. K. Kim, A. Koitzsch, M. Knupfer, M. S. Golden, J. Fink, M. Eschrig, H. Berger, and R. Follath, Phys. Rev. Lett. **90**, 207001 (2003).